Evolution of supraglacial lakes on the Larsen B ice shelf in the decades before it collapsed

Evolution of supraglacial lakes on the Larsen B ice shelf in the decades before it collapsed

A. A. Leeson[1,2], E. Forster[2], A. Rice[3], N. Gourmelen[4] and J. M. van Wessem[5]

[1]Data Science Institute, Lancaster University, LA1 4YW.

[2]Lancaster Environment Centre, Lancaster University, LA1 4YW.

[3]School of Mathematics and Statistics, Lancaster University. LA1 4YF.

[4]School of Geosciences, University of Edinburgh, EH9 3FE

[5]Institute for Marine and Atmospheric research Utrecht (IMAU), University of Utrecht, Utrecht, The Netherlands

Corresponding author: Amber Leeson (a.leeson@lancaster.ac.uk)

Key Points:

- Supraglacial lakes spread southwards on the Larsen B ice shelf in the two decades preceding its collapse at a rate commensurate with meltwater saturation of its surface.
- There was no trend in lake size during this time, suggesting an active surface drainage network that evacuated excess water off the shelf.
- Lakes mostly re-freeze in winter but a few lakes drain. Those that drain seem to be associated with ice break up 2-4 years later.

Abstract

The Larsen B ice shelf collapsed in 2002 losing an area twice the size of Greater London to the sea (3000 km^2), in an event associated with widespread supraglacial lake drainage. Here, we use optical and radar satellite imagery to investigate the evolution of the ice shelf's lakes in the decades preceding collapse. We find 1) that lakes spread southwards in the preceding decades at a rate commensurate with meltwater saturation of the shelf surface, 2) no trend in lake size, suggesting an active supraglacial drainage network which evacuated excess water off the shelf and 3) lakes mostly re-freeze in winter but the few lakes that do drain are associated with ice break up 2-4 years later. Given the relative scale of lake drainage and shelf break up, however, it is not clear from our data whether lake drainage is more likely a cause, or an effect, of ice shelf collapse.

1 Introduction

The Antarctic Peninsula (AP) has experienced extreme warming in the mid to late 20th Century, with air temperatures increasing by almost 2.5°C (e.g. Vaughan and Doake 1996, Skvarca et al., 1999), up to ~1990 (Turner, Lu et al. 2016). This has been linked to thinning and loss of the AP's ice shelves (e.g. Morris and Vaughan 2003, Shepherd et al., 2003). During the 1990's, the Larsen B ice shelf (LBIS) began to shrink, culminating in its eventual collapse in 2002 (e.g. Scambos et al., 2003, Glasser and Scambos 2008). Since then, the glaciers which formerly fed into LBIS have accelerated between two- and eight-fold, following the removal of buttressing forces formerly provided by the shelf (e.g. Rignot et al., 2004, Scambos et al., 2004). Through this mechanism, ~9 Gt yr^{-1} of grounded ice has been lost to the sea, accounting for one third of all ice loss observed from the AP since 2002 (Berthier et al., 2012).

Supraglacial lakes (SGLs) form in surface depressions from ponded melt water. They are a component of the ice surface hydrological network which also includes streams and rivers (Glasser and Scambos, 2008). This network is important because it can route surface meltwater into lakes (Stokes et al., 2019), moulins (Langley et al., 2016) or off of the ice into the ocean (Bell et al., 2017). By exporting meltwater off of the ice, supraglacial streams can strengthen ice shelves (ibid). SGLs however, have been implicated in ice shelf breakup (e.g. Banwell and MacAyeal, 2015). Widespread SGL coverage was observed on the Prince Gustav and Larsen A ice shelves before their failure in the mid-1990s (e.g. Cooper 2009), and lakes on the LBIS were observed to drain just before its collapse (Scambos et al., 2003). SGLs can drain laterally through supraglacial streams (Kingslake et al., 2015) or vertically via hydrofracture; when water-filled crevasses propagate through the full ice thickness (MacAyeal et al., 2003, Krawczynski et al., 2009). Through repeated filling and draining, SGLs induce localized flexure of the ice shelf. It is thought that this can produce fractures that can cause neighboring lakes to drain in a chain reaction, leading ultimately to ice shelf disintegration (Banwell and MacAyeal 2015).

Since much of Antarctica is fringed by floating ice shelves that provide important buttressing to grounded ice flow (Fürst et al., 2016, Goldberg et al., 2019), it is important to understand the contribution of supraglacial hydrology to ice shelf stability. Here we investigate the potential role of SGLs in the collapse of LBIS by analyzing their evolution from 1979 to 2002 (Figure 1) using a combination of optical and synthetic aperture radar (SAR) satellite imagery (supporting table 1).

2 Data and Methods

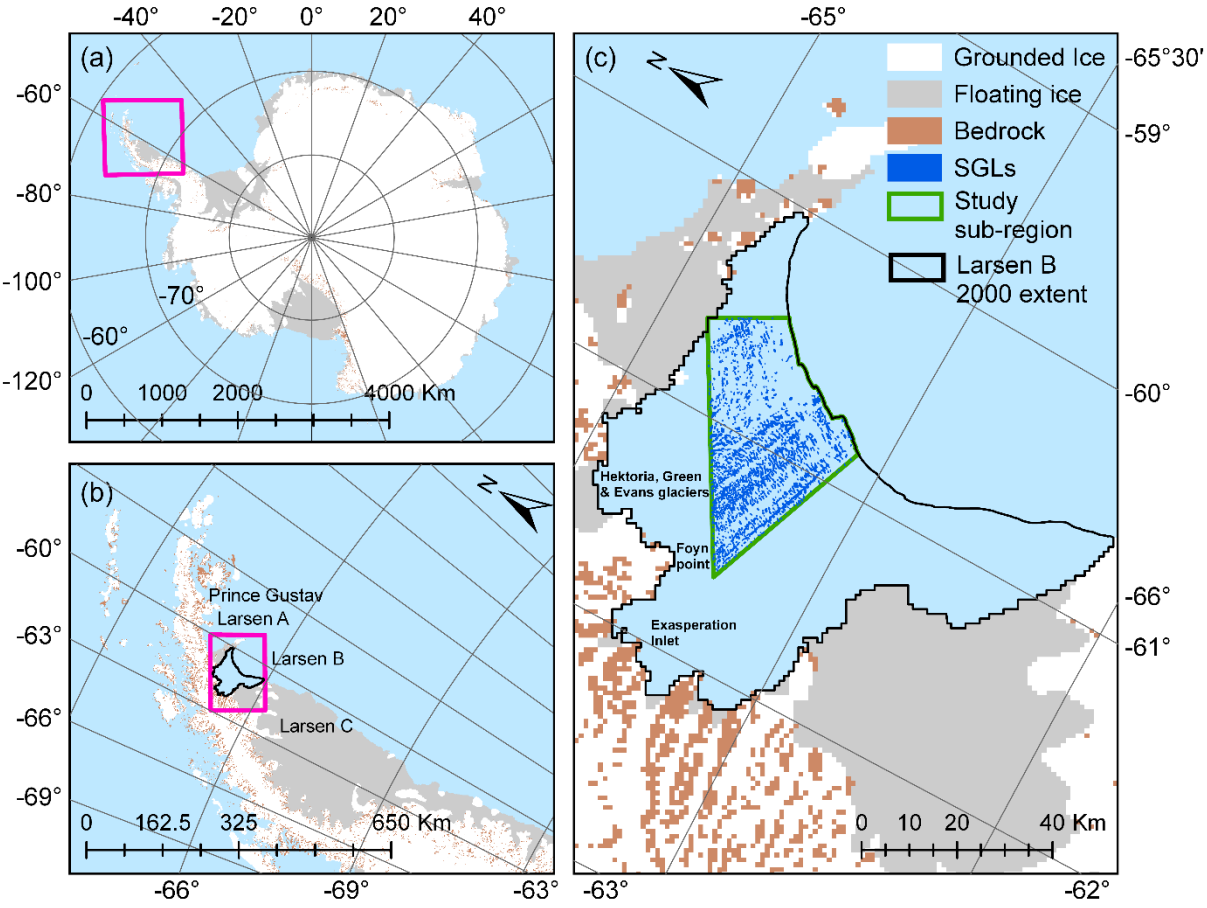

Figure 1: Map of study area. (a) Antarctica. Pink denotes location of: (b) Antarctic Peninsula, portion of the Larsen B ice shelf lost in 2002 outlined in black. Pink denotes location of: (c) Larsen B embayment. Bedrock and grounded/floating ice from Bedmap2 (Fretwell, Pritchard et al. 2013).

2.1 Satellite Data

Here we use all available, high quality satellite images acquired between November and March during 1979 and 2002 over the LBIS. These data are 8 optical satellite images acquired for 7 separate years by NASA/USGS's Landsat series and 13 Synthetic Aperture Radar (SAR) images acquired for 6 separate years by ESA's European Remote Sensing (ERS) platforms (supporting table S1). The SAR signature of lakes changes annually from dark lakes against a light background in winter to bright lakes against a dark background in summer (supporting text S2.2). Here, we choose the summer SAR image in which lakes were clearest for each of the years we have data for quantitative analysis (section 3.2); these were mostly acquired between mid-January and mid-February. In order to compare lake characteristics between years, ERS data are radiometrically calibrated and georeferenced (Nagler et al., 2016). SGLs are then manually delineated in ERS and automatically and manually delineated in Landsat (supporting text S2.1 and S2.2). We quantify uncertainty associated with using two different sensors by digitizing lakes in a 52 km^2 sample area in Landsat and ERS images acquired 2 days apart. We find that 7% more lakes are identified in ERS images, lakes are 16% larger on average in Landsat and cover an 8% greater area (supporting text S2.3).

To account for the fact that lake covered area changed during our study period, and to provide a fair comparison between Landsat and ERS, we subsampled our study area to that covered by lakes in 1988, omitting regions where lakes were unclear in ERS due to speckle noise (granular interference). We use a partially cloudy Landsat image from 9th February 1990 in section 3.2. We account for the cloud cover by calculating the change in lake characteristics in the cloud free area with respect to the Landsat image captured on 19th January 1988, then applying the relative change to the cloud covered portion. Finally, we use a radiative transfer model (supporting text S2.3) to compare lake depth and volume between two cloud-free Landsat images acquired on the 19th January 1988 and 21st February 2000.

2.2 Meteorological data

We contextualize our findings with simulated meteorology and simulated firn conditions from the Regional Atmospheric Climate Model (RACMO2). Details of the model are found in van Wessem et al., (2016) and summarized here. RACMO2 combines the High Resolution Limited Area Model (HIRLAM) with the European Centre for Medium-range Weather Forecasts (ECMWF) Integrated Forecast System (IFS) and has been adapted for use over the large ice sheets of Greenland and Antarctica. ERA-Interim re-analysis data are used for forcing at lateral boundaries and surface topography is based on a combination of the 100 m and 1 km digital elevation models from Cook et al., (2012) and Bamber et al., (2009), respectively. In previous work we found that the model systematically underestimates air temperature by 1.82^{o}C over LBIS, (Leeson et al., 2017) and correct for this here by adding 1.82^{o}C to all temperature estimates.

4 Results

3.1 Southward spreading of lakes

Using images from Landsat and ERS (supporting table S1) acquired in nine of the years between 1979-2002, we quantify changes in lake covered area by manually delineating the southernmost boundary of lake covered area in ArcGIS (Figure 2). In 1979, lakes are confined to the Hektoria/Green/Evans glaciers domain north of Foyn Point (locations identified in Figure 1). By the austral summer of 1987/1988 lakes had spread to the north of Exasperation Inlet (noted in Skvarca et al., 1999) and in 1993 had reached its southern boundary. From ~1996, lakes begin to encroach upon the shelf from the south and by 2002, covered almost the entire area. This corresponds to a southward spreading rate of 2.59 km (0.02^{o}) per year between 1979-2002. This is split into two different periods with a threefold speed up in spreading rate after 1993 (0.01^{o} per year 1979-1990 and 0.03^{o} per year 1993-2002). According to simulations performed by RACMO2 over this region, 1993 was a very high melt year (more than twice as much melting as the 1990-1999 average, Leeson et al., 2017) and a year with particularly low minimum firn air content on the portion of the shelf lost in 2002 (Figure 2l). This suggests that high melting in this year saturated the ice shelf's firn pack, thereby preconditioning it for SGL formation in subsequent years (Kuipers Munneke et al., 2014). We also note that the retreat of the ice shelf (e.g. Kulessa et al., 2014) is clear in the ERS images after 1993, with the shelf progressively shrinking down to its pre-collapse extent by 2000.

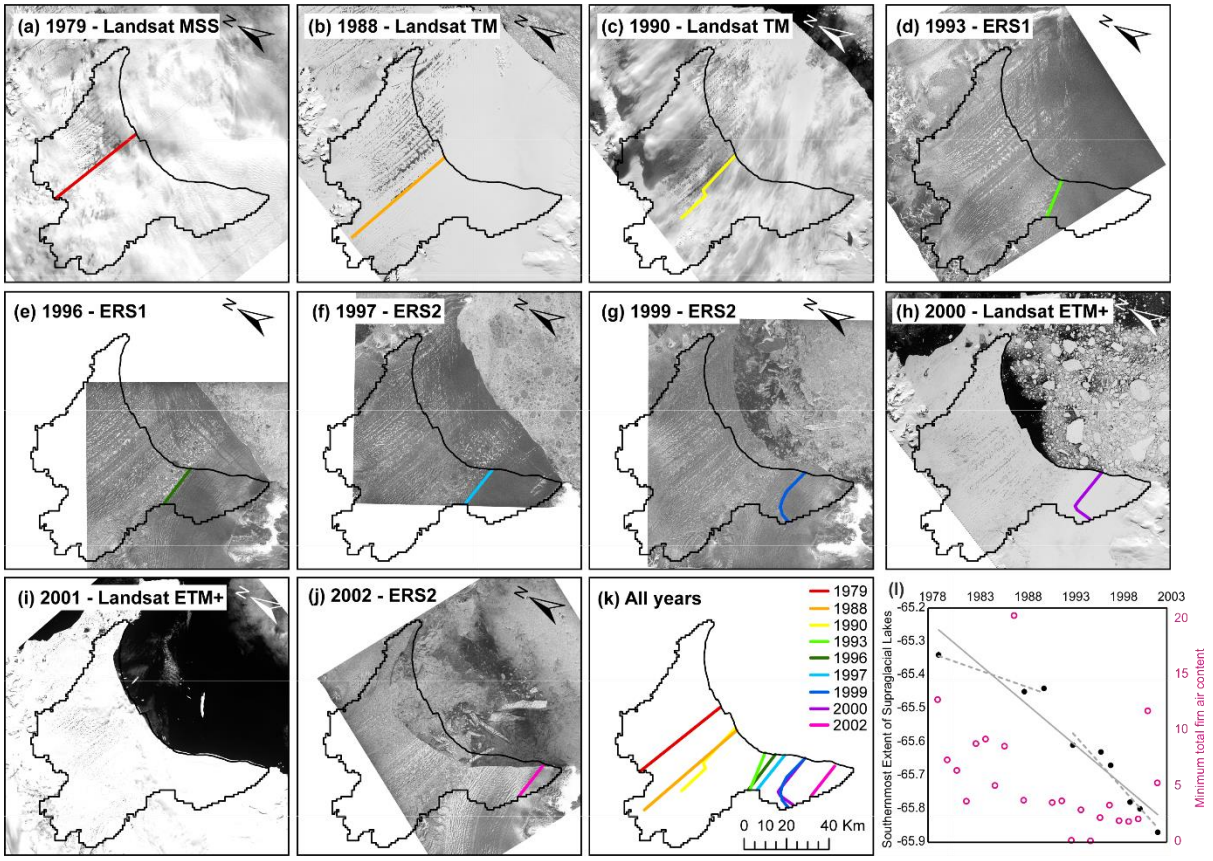

Figure 2: Southward spreading of supraglacial lakes on LBIS between 1979-2002. (a)-(j) satellite image of LBIS acquired in year indicated. Colored lines denote southern border of lake covered area. Black outline denotes portion of shelf lost in 2002. (k) these data on a single map. (l) time series of these data (black) together with corresponding minimum firn air content from RACMO2 (pink) of portion of shelf lost in 2002. Solid line denotes a linear fit to all time points. Dashed lines indicate linear fits to 1979-1990 and 1993-2002 inclusive.

3.2 Changes in lake characteristics and relationship with climate

We assess the variability in lake number, size and total area in our study area between 1988-2002 and investigate potential relationships to climate. The presence of clouds in some Landsat images precluded their use in this analysis, reducing our sample to seven individual years across the 23-year study period. Using these data, we found no noticeable trend in lake characteristics (Figure 3); lake number, size and total area within our sample did not increase. Variability was reasonably high in each case with 1993 and 2000 acting as end members for each parameter with fewer, larger lakes in 1993 (335 lakes, mean area 0.64 km^2) and an abundance of small lakes in 2000 (1170 lakes, mean area 0.07 km^2). We attribute this to topography; small lakes coalesce in high melt years to form fewer, larger lakes. Using regression analysis we found that summer (DJF) melting simulated by RACMO2 best explains inter-annual variability in mean and total lake area (supporting text S5). Mean and total lake area are strongly correlated with DJF melting ($r=0.95$, $p<0.01$ and $r=0.77$, $p=0.01$, respectively), in good agreement with Langley et al., (2016). We note that these patterns hold despite images being acquired on different days into the melt season. This suggests that lakes reach their maximum size by mid-January and do not grow or shrink significantly between then and mid-February. Lake number is weakly anti-correlated with DJF melting ($r=-0.58$, $p=0.18$), suggesting that other factors, e.g. the time of year, act as a more important control (see supplementary text S5).

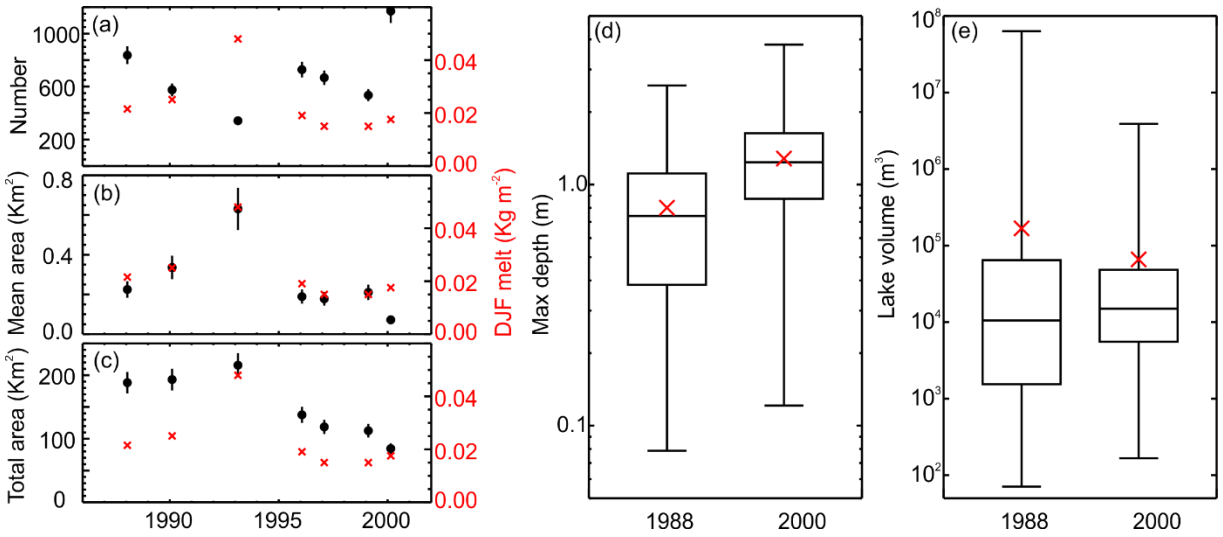

Figure 3. Temporal variability in lake characteristics. (a)–(c) black circles indicate lake characteristic, error bars indicate uncertainty due to different sensors (section 2.1). Red crosses denote total summer (DJF) melting over portion of shelf lost in 2002 according to RACMO2. (d)-(e) show box and whisker plots of lake depth and volume retrieved from Landsat images acquired in 1988 and 2000. Mean values are indicated by red crosses.

We compare lake depth and volume between two cloud-free Landsat images acquired towards the beginning (19th January 1988) and end (21st February 2000) of our study period (Figure 3d,e). There are notable differences in both depth and volume between these images, despite similar predicted melt amounts in each year. Lakes hold more water in 1988 with a mean volume of 1.7 x 10^5 m^3 compared to 0.6 x 10^5 m^3 in 2000. This is not surprising since mean lake area is twice as large in 1988. This is likely a result of lakes refreezing; the 2000 image was captured a full month later than the 1988 image. More interesting however is that in 2000, lakes are more than 50% deeper than in 1988 with average maximum depths of 1.28 m and 0.8 m, respectively. This is interesting because, for a fixed surface topography, one might expect the larger lakes to be deeper. This suggests that the surface topography of the ice shelf is not fixed, and that the depressions in which lakes form deepened between 1988 and 2000. This is despite the likely onset of refreezing prior to the date of acquisition of the 2000 image and is spatially independent (supporting figure S7).

3.3 Evidence for lake drainage

In our combined ERS-Landsat record we find evidence for lakes refreezing, vertical drainage and lateral drainage.

Prior to 2002, lakes tend to persist through the winter without draining; for example ERS images acquired in March 1996, 1997 and November 1996 show lakes on the LBIS after/before the DJF melt season. A cloud-free Landsat image acquired on the 1st March 1986 shows no lakes, rather it shows abundant snow which suggests that the surface of the lakes has frozen over, and they have subsequently been buried. Buried lakes are visible in ERS because of the capability of radar to penetrate snow (Johansson and Brown 2013). In ERS imagery from 1996, ~100 lakes located in the northernmost part of the region are visible on February 29th but not visible on March 24th (Figure 4). Since RACMO2 shows that the air temperature was consistently below zero between these dates it is reasonable to assume that these lakes fully refroze. Similar numbers of lakes in the 21st February 2000 Landsat image appear to be refreezing/refrozen, based on their similarity to refreezing lakes in previous

work (e.g. Langley et al., 2016). This is supported by the temperature data; in the seven days prior to image acquisition, mean temperatures across most of the ice shelf were below zero. In both cases, refrozen lakes seem concentrated towards the ice margin, likely because temperatures are colder there beyond the influence of warm föhn wind (e.g. Cape et al., 2015, Leeson et al, 2017).

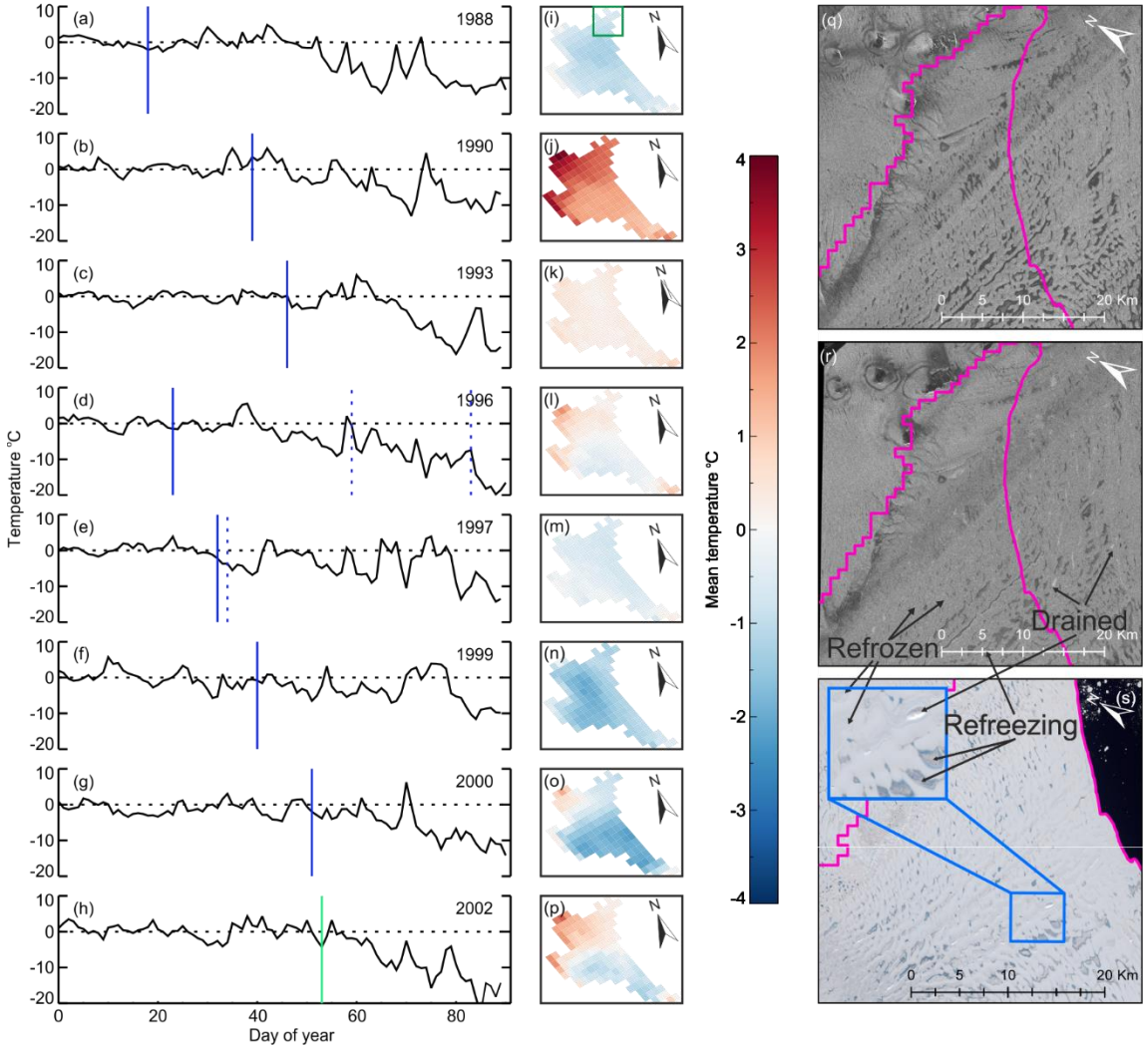

Figure 4: Evidence for lake refreezing. (a)–(h): time series of daily mean temperature (simulated by RACMO2) over portion of shelf lost in 2002. Dates of acquisition of main images used in our analysis are indicated by solid blue bars, other images referred to in text are indicated by dashed blue bars. Solid green bar indicates approximate date of ice shelf collapse. (i)–(p): mean temperature over seven days preceding main image acquisition. Green square in (i) identifies area in (q)-(r). (q)–(r) ERS images acquired on February 29th and March 24th 1996. (s) Landsat image acquired 21st February 2000. Pink outline in (q)-(s) bounds now-missing portion of ice shelf.

We see evidence for lake drainage in years before 2000, mainly on portions of the ice shelf which broke off before the main collapse. In 1996, a cluster of ~10 lakes disappear mid-melt season between ERS images captured on January 25th and February 29th (Figure 5). Similarly, a cluster of ~6 lakes disappear between 2nd February 1997 (ERS) and 4th February 1997 (Landsat). In both cases the disappeared lakes are surrounded by visible lakes, suggesting that they did not refreeze. In the case of the 1996 images, the drained lakes appear slightly brighter than the surrounding surface (signature also noted in Miles et al., 2017). We

see more evidence (~20 lakes) of this signature in an ERS image captured March 24th 1996 (Figure 4r), mainly on the portion of LBIS lost before 2000. The drained lakes are not particularly noteworthy in that their area and shape appear consistent with surviving lakes. This suggests that their drainage was glaciologically determined i.e. initiated as a result of local perturbations in ice flow. We note that this period in time has been associated with LBIS speed-up in other studies (e.g. Kulessa et al., 2014), and that the drained lakes are oriented perpendicular to the direction of flow, both of which support this inference. Since these lakes are grouped, it is possible that a single glaciologically-driven event may have triggered a small scale chain reaction draining neighboring lakes (e.g. Banwell et al., 2013), however higher resolution observations in time are needed to confirm this.

In the image captured 21st February 2000 we see ~19 shapes characterized by light and dark patterns consistent with steep-sided topographic depressions (e.g. Figure 4s). We interpret these to be lakes which have drained, supporting previous findings (e.g. Glasser and Scambos 2008). Since we have a contemporaneous ERS image acquired on 27th February 2000 we examine the locations of these lakes in SAR and identify a possible signature (supporting section S9). We see evidence of this signature in ERS images acquired in 2002 around the time of shelf break up, however the images are too noisy and the signature insufficiently clear to draw any conclusions. In our record we also have two relatively cloud-free Landsat images from the early part of the 2001/2002 melt season captured 15th and 31st December 2001. These images show lakes present on 15th December that are not present on 31st December (Figure 5c). Since this coincides with downstream lakes increasing in size between the two dates, and temperatures increasing rather than decreasing, we interpret this to be evidence of lateral lake drainage (e.g. Kingslake et al., 2015).

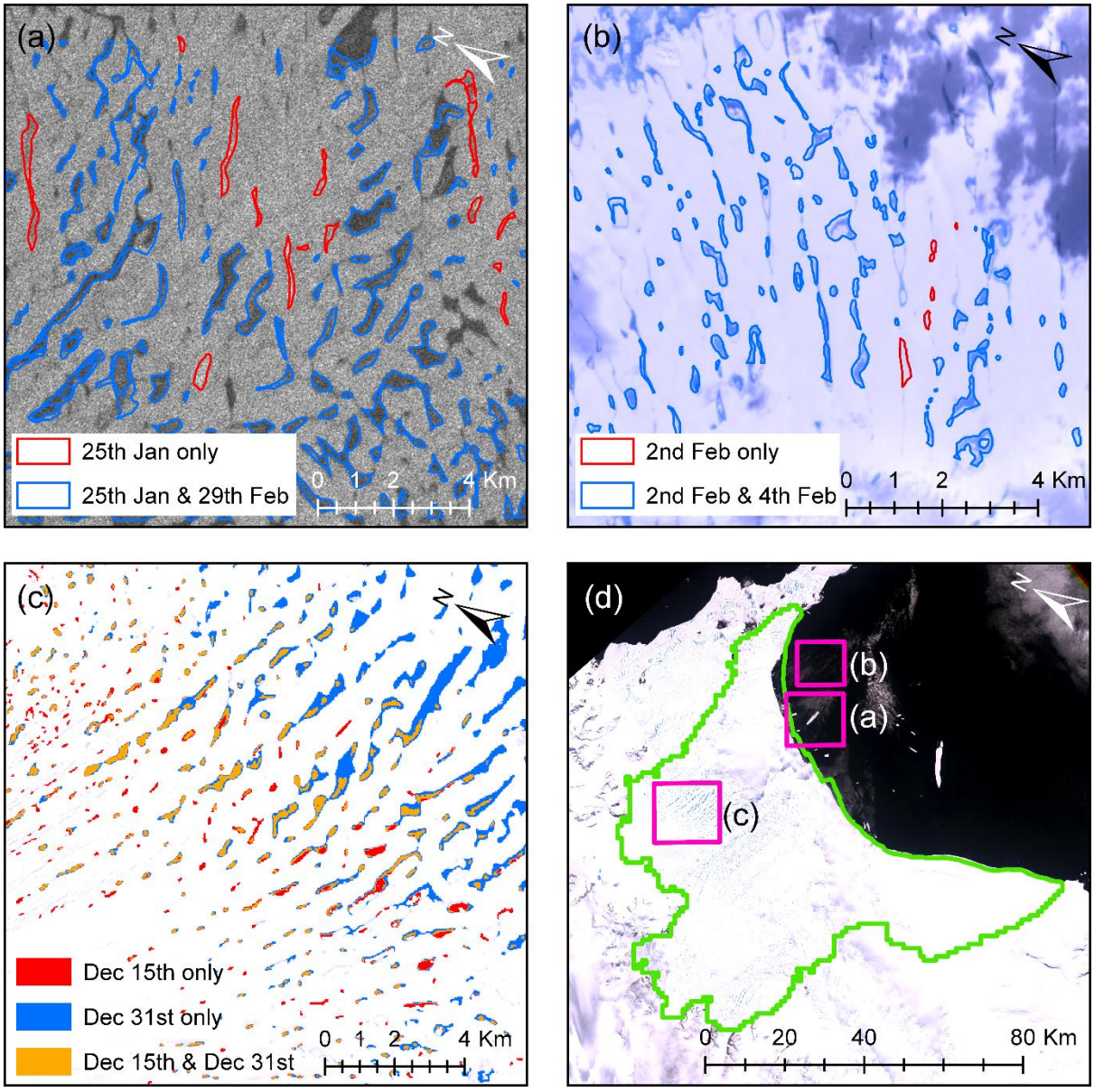

Figure 5: Evidence for lake drainage. (a) ERS image acquired 29th February 1996. Lakes delineated from this image (blue) and from ERS image acquired 25th January 1996 (blue+red).(b) True colour Landsat TM image acquired 4th February 1997. Lakes delineated from this image (blue) and from ERS image acquired 2nd February 1997 (blue+red). (c) Landsat ETM+ image acquired 31st December 2001. Lakes delineated from same (blue), lakes delineated from Landsat ETM+ image acquired 15th December 2001 (red), areas of lake that appear in both images (orange). (d) True colour Landsat ETM+ image acquired 21st December 2001. Green denotes now-missing portion of the ice shelf. Pink boxes outline locations in (a)-(c).

5 Conclusions

We use SAR and optical satellite imagery to investigate the evolution of SGLs on the LBIS prior to its collapse and find that lakes spread southwards at a rate consistent with firn air depletion, covering almost the entire ice shelf by 2002. This is consistent with previous studies which suggest both a temperature-dependent latitudinal 'limit of viability' for ice shelves (Morris and Vaughan 2003) and a firn-density based metric of ice shelf vulnerability (Alley et al. 2018). We note in particular that 1993 and 1995 were the years of lowest firn air

content in our record, directly preceding the beginning of the ice shelf break-up in 1995. Notably, RACMO2 does not simulate a temperature or surface melt trend during this period (Leeson et al., 2017). This suggests that ice shelf vulnerability is cumulative, and that accurate measurements and models of meltwater retention in firn are needed in order to assess the risk of collapse of other ice shelves.

We find that, according to our data, there was no trend in lake area over the 1979-2002 study period and that lake area is best described by seasonal melt volume. This is interesting because such behavior reflects an inter-connected hydrological network where lake size is a function of throughput rate rather than total abundance of water. We see evidence for some linear meltwater features that terminate at crevasses or the shelf terminus, which could provide a mechanism for meltwater export off-shelf (supplementary figure S11). This supports the work of Kingslake et al., (2017) and Bell et al., (2017) who characterize Antarctic ice shelf hydrology as a dynamic system where excess meltwater is exported e.g. off the ice shelf, as opposed to being stored locally. Our findings suggest that the LBIS exhibited a combination of local storage (in lakes) and meltwater export, which may explain why it was able to support an abundant population of lakes for several decades before it finally collapsed. We also find that lakes get deeper over time. Since this holds across a wide area, and we do not see evidence of repeated widespread draining, we attribute this to enhanced ablation at the lake bed (Buzzard, Feltham et al. 2018) as opposed to a viscous response to successive fill/drain cycles (Banwell et al., 2013).

At the end of the melt season, we find that most lakes refreeze but a small proportion drain. Specifically we see evidence for ~30 lakes draining prior to March 24th 1996. These potential drained lakes are mainly located on floating ice which broke off between 1996 and 2000. The first time we see evidence for multiple lakes draining on the portion of ice shelf lost in 2002 is in 2000, where we see evidence for ~20 drained lake basins. Thus we find that, in our dataset, floating ice on which SGLs drain breaks up 2-4 years after drainage is first observed. We note however that the number of observed lake drainages is small in both cases, relative to the large size of the broken off area. As such, it is not clear from these data whether the lake drainages were a cause, or rather an effect, of the LBIS break-up.

Data availability

Landsat data is available at: https://earthexplorer.usgs.gov/. ERS data is available at https://earth.esa.int/web/guest/data-access. RACMO2 data are available from co-author JMvW. Yearly climate variables are available at: https://www.projects.science.uu.nl/iceclimate/publications/data/2018/index.php. Our lake shapefiles and depth data are archived at https://doi.org/10.5285/90cde9d9-bc80-41d4-8102-d3d0bb58a029.

References

Alley, K. E., T. A. Scambos, J. Z. Miller, D. G. Long and M. MacFerrin (2018). "Quantifying vulnerability of Antarctic ice shelves to hydrofracture using microwave scattering properties." Remote Sensing of Environment 210: 297-306.

Bamber, J. L., J. L. Gomez-Dans and J. A. Griggs (2009). "A new 1 km digital elevation model of the Antarctic derived from combined satellite radar and laser data - Part 1: Data and methods." Cryosphere 3(1): 101-111.

Banwell, A. F. and D. R. Macayeal (2015). "Ice-shelf fracture due to viscoelastic flexure stress induced by fill/drain cycles of supraglacial lakes." Antarctic Science 27(6): 587-597.

Banwell, A. F., M. Caballero, N. S. Arnold, N. F. Glasser, L. Mac Cathles and D. R. MacAyeal (2014). "Supraglacial lakes on the Larsen B ice shelf, Antarctica, and at Paakitsoq, West Greenland: a comparative study." Annals of Glaciology 55(66): 1-8. Citation in supplementary material.

Banwell, A. F., D. R. MacAyeal and O. V. Sergienko (2013). "Breakup of the Larsen B Ice Shelf triggered by chain reaction drainage of supraglacial lakes." Geophysical Research Letters 40(22): 5872-5876.

Bell, R. E., W. Chu, J. Kingslake, I. Das, M. Tedesco, K. J. Tinto, C. J. Zappa, M. Frezzotti, A. Boghosian and W. S. Lee (2017). "Antarctic ice shelf potentially stabilized by export of meltwater in surface river." Nature 544: 344.

Berthier, E., T. A. Scambos and C. A. Shuman (2012). "Mass loss of Larsen B tributary glaciers (AP) unabated since 2002." Geophysical Research Letters 39: 6.

Bindschadler, R. and P. Vornberger (1992). "Interpretation of SAR imagery of the Greenland ice-sheet using coregistered tm imagery." Remote Sensing of Environment 42(3): 167-175. Citation in supplementary material.

Box, J. E. and K. Ski (2007). "Remote sounding of Greenland supraglacial melt lakes: implications for subglacial hydraulics." Journal of Glaciology 53(181): 257-265. Citation in supplementary material.

Bruzzone, L., M. Marconcini, U. Wegmuller and A. Wiesmann (2004). "An advanced system for the automatic classification of multitemporal SAR images." Ieee Transactions on Geoscience and Remote Sensing 42(6): 1321-1334. Citation in supplementary material.

Buzzard, S. C., D. L. Feltham and D. Flocco (2018). "A Mathematical Model of Melt Lake Development on an Ice Shelf." Journal of Advances in Modeling Earth Systems 10 (2): 262-283.

Cape, M. R., M. Vernet, P. Skvarca, S. Marinsek, T. Scambos and E. Domack (2015). "Foehn winds link climate-driven warming to ice shelf evolution in Antarctica." Journal of Geophysical Research-Atmospheres 120(21): 11037-11057.

Chander, G., B. L. Markham and D. L. Helder (2009). "Summary of current radiometric calibration coefficients for Landsat MSS, TM, ETM+, and EO-1 ALI sensors." Remote Sensing of Environment 113(5): 893-903. Citation in supplementary material.

Cook, A. J., T. Murray, A. Luckman, D. G. Vaughan and N. E. Barrand (2012). "A new 100-m Digital Elevation Model of the AP derived from ASTER Global DEM: methods and accuracy assessment." Earth System Science Data 4(1): 129-142.

Cooper, A. P. R. (2009). "Historical observations of Prince Gustav Ice Shelf." Polar Record 33(187): 285-294.

Fretwell, P. et al., (2013). "Bedmap2: improved ice bed, surface and thickness datasets for Antarctica." The Cryosphere 7(1): 375-393.

Fürst, J. J., G. Durand, F. Gillet-Chaulet, L. Tavard, M. Rankl, M. Braun and O. Gagliardini (2016). "The safety band of Antarctic ice shelves." Nature Climate Change 6: 479.

Glasser, N. F. and T. A. Scambos (2008). "A structural glaciological analysis of the 2002 Larsen B ice-shelf collapse." Journal of Glaciology 54(184): 3-16.

Goldberg, D. N., N. Gourmelen, S. Kimura, R. Millan and K. Snow (2019). "How Accurately Should We Model Ice Shelf Melt Rates?" Geophysical Research Letters 46(1): 189-199.

Jansen, D., B. Kulessa, P. R. Sammonds, A. Luckman, E. C. King and N. F. Glasser (2010). "Present stability of the Larsen C ice shelf, AP." Journal of Glaciology 56(198): 593-600.

Johansson, A. M. and I. A. Brown (2013). "Adaptive Classification of Supra-Glacial Lakes on the West Greenland Ice Sheet." Selected Topics in Applied Earth Observations and Remote Sensing, IEEE Journal of PP(99): 1-10.

Johansson, A. M. and I. A. Brown (2012). "Observations of supra-glacial lakes in west Greenland using winter wide swath Synthetic Aperture Radar." Remote Sensing Letters 3(6): 531-539.

Johansson, M., I. A. Brown and P. Jansson (2011). Multi-temporal, multi-sensor investigations of supra-glacial lakes on the Greenland Ice Sheet. ESA Living Planet Symposium: 28 June - 2 July 2010, Bergen, Norway. H. Lacoste-Francis. Noordwijk, ESA (European Space Agency). Citation in supplementary material.

Kingslake, J., J. C. Ely, I. Das and R. E. Bell (2017). "Widespread movement of meltwater onto and across Antarctic ice shelves." Nature 544: 349.

Kingslake, J., F. Ng and A. Sole (2015). "Modelling channelized surface drainage of supraglacial lakes." Journal of Glaciology 61(225): 185-199.

Krawczynski, M. J., M. D. Behn, S. B. Das and I. Joughin (2009). "Constraints on the lake volume required for hydro-fracture through ice sheets." Geophysical Research Letters 36: 5.

Kuipers Munneke, P., S. R. M. Ligtenberg, M. R. van den Broeke and D. G. Vaughan (2014). "Firn air depletion as a precursor of Antarctic ice-shelf collapse." Journal of Glaciology 60(220): 205-214.

Kulessa, B., D. Jansen, A. J. Luckman, E. C. King and P. R. Sammonds (2014). "Marine ice regulates the future stability of a large Antarctic ice shelf." Nature Communications 5(1): 3707.

Langley, E. S., A. A. Leeson, C. R. Stokes and S. S. R. Jamieson (2016). "Seasonal evolution of supraglacial lakes on an East Antarctic outlet glacier." Geophysical Research Letters 43(16): 8563-8571.

Leeson, A. A., A. Shepherd, S. Palmer, A. Sundal and X. Fettweis (2012). "Simulating the growth of supraglacial lakes at the western margin of the Greenland ice sheet." Cryosphere 6(5): 1077-1086.

Leeson, A. A., J. M. Van Wessem, S. R. M. Ligtenberg, A. Shepherd, M. R. Van Den Broeke, R. Killick, P. Skvarca, S. Marinsek and S. Colwell (2017). "Regional climate of the Larsen B embayment 1980-2014." Journal of Glaciology 63(240): 683-690.

MacAyeal, D. R., T. A. Scambos, C. L. Hulbe and M. A. Fahnestock (2003). "Catastrophic ice-shelf break-up by an ice-shelf-fragment-capsize mechanism." Journal of Glaciology 49(164): 22-36.

Maritorena, S., A. Morel and B. Gentili (1994). "Diffuse-reflectance of oceanic shallow waters - influence of water depth and bottom albedo." Limnology and Oceanography 39(7): 1689-1703. Citation in supplementary material.

Miles, K. E., I. C. Willis, C. L. Benedek, A. G. Williamson and M. Tedesco (2017). "Toward Monitoring Surface and Subsurface Lakes on the Greenland Ice Sheet Using Sentinel-1 SAR and Landsat-8 OLI Imagery." Frontiers in Earth Science 5(58).

Morris, E. M. and D. G. Vaughan (2003). Spatial and temporal variation of surface temperature on the AP and the limit of viability of ice shelves. AP Climate Variability: Historical and Paleoenvironmental Perspectives. E. Domack, A. Leventer, A. Burnett et al. 79: 61-68.

Nagler, T., H. Rott, E. Ripper, G. Bippus and M. Hetzenecker (2016). "Advancements for Snowmelt Monitoring by Means of Sentinel-1 SAR." Remote Sensing 8(4).

Rignot, E., G. Casassa, P. Gogineni, W. Krabill, A. Rivera and R. Thomas (2004). "Accelerated ice discharge from the AP following the collapse of Larsen B ice shelf." Geophysical Research Letters 31(18).

Scambos, T., C. Hulbe and M. Fahnestock (2003). Climate-induced ice shelf disintegration in the AP. AP Climate Variability: Historical and Paleoenvironmental Perspectives. E. Domack, A. Leventer, A. Burnett et al. Washington, Amer Geophysical Union. 79: 79-92.

Scambos, T. A., J. A. Bohlander, C. A. Shuman and P. Skvarca (2004). "Glacier acceleration and thinning after ice shelf collapse in the Larsen B embayment, Antarctica." Geophysical Research Letters 31(18): 4.

Scambos, T. A., C. Hulbe, M. Fahnestock and J. Bohlander (2000). "The link between climate warming and break-up of ice shelves in the AP." Journal of Glaciology 46(154): 516-530.

Shepherd, A., D. Wingham, T. Payne and P. Skvarca (2003). "Larsen Ice Shelf Has Progressively Thinned." Science 302(5646): 856-859.

Skvarca, P., W. Rack and H. Rott (1999). 34 year satellite time series to monitor characteristics, extent and dynamics of Larsen B Ice Shelf, AP. Annals of Glaciology, Vol 29, 1999. T. H. Jacka. 29: 255-260.

Skvarca, P., W. Rack, H. Rott and T. I. Y. Donangelo (1999). "Climatic trend and the retreat and disintegration of ice shelves on the AP: an overview." Polar Research 18(2): 151-157.

Smith, R. C. and K. S. Baker (1981). "Optical-properties of the clearest natural-waters (200-800 nm)." Applied Optics 20(2): 177-184. Citation in supplementary material.

Sneed, W. A. and G. S. Hamilton (2007). "Evolution of melt pond volume on the surface of the Greenland Ice Sheet." Geophysical Research Letters 34(3): 4.

Turner, J., H. Lu, I. White, J. C. King, T. Phillips, J. S. Hosking, T. J. Bracegirdle, G. J. Marshall, R. Mulvaney and P. Deb (2016). "Absence of 21st century warming on Antarctic Peninsula consistent with natural variability." Nature 535(7612): 411-415.

van Wessem, J. M., S. R. M. Ligtenberg, C. H. Reijmer, W. J. van de Berg, M. R. van den Broeke, N. E. Barrand, E. R. Thomas, J. Turner, J. Wuite, T. A. Scambos and E. van Meijgaard (2016). "The modelled surface mass balance of the AP at 5.5km horizontal resolution." Cryosphere 10(1): 271-285.

Vaughan, D. G. and C. S. M. Doake (1996). "Recent atmospheric warming and retreat of ice shelves on the AP." Nature 379(6563): 328-331.